

A Novel Multi-scale 3D Area Morphological Filtering Method for Airborne LiDAR Building Extraction

Cao Zhimin, Wu Yun

*School of Electronic Science, North-East Petroleum University, Daqing, China
dahai0464@sina.com*

Abstract

Automatic building extraction is one of the most important issues in the fields of geoscience and remote sensing. In this letter, by introducing the idea of area morphology to the analysis of 3-D point clouds, a novel approach for automatic building extraction from airborne LiDAR data was proposed. At first, single scale area opening and area closing operator was used to produce normalized point clouds. With the normalized point clouds as input, multi-scale area morphology was employed to obtain connected regions, and then tree points were removed by PCA based local structural analyzing technique. Finally, building regions were extracted by analyzing geometry properties of the obtained connected regions without tree points. Experiments for different terrains were conducted. And the corresponding experimental results are very promising.

Keywords: *building extraction, area morphology, airborne LiDAR*

1. Introduction

Building extraction has been one of the most important and challenging tasks for applications such as 3-D city modeling, infrastructure planning and disaster emergency response. Recently, with the capability of directly providing dense accurate geo-referenced 3-D point clouds, airborne LiDAR has become a popular used alternative to conventional techniques for automatic building extraction.

Many approaches have been proposed to automatically extract buildings from airborne LiDAR data in the past decade [1-4] (and their references). In general, there are mainly two strategies for extracting buildings using LiDAR data. The first one is to analyze raw point clouds or the corresponding mesh structure directly. And the second one is to rasterize the raw LiDAR data onto a regular sampled image (*i.e.*, DSM), and then to analyze the DSM or nDSM for extracting buildings. No matter which strategy is employed, segmentation is always the first step [1], *i.e.*, acquiring connected regions from the input data. Sampath and Shan [2] employed 2-D Voronoi polygons to define the neighborhood of a given point, and then structural features for each point were analyzed by using PCA based structural analysis technique to segment raw LiDAR data into planar and non-planar points. RANSAC plane fitting or 3D Hough Transform plane extraction can also be used to segment the raw LiDAR data into planar and non-planar regions [3]. E Aparecida dos Santos Galvanin [4] translated the raw LiDAR data into a regular sampled DSM, and then Markov Random Filed technique was used to analyze the segmented aboveground regions. Even though there are still many corresponding researches are carrying out to enhance the performance of automatic building extraction from airborne LiDAR data, heavy computational burden for the first strategy and information loss during rasterization for the second strategy are the main problems far from solved.

Recently, results given by some hierarchical and multi scale approaches seem to be very promising [5-9]. T. Thuy Vu *et al* [5] introduced grayscale area opening and closing operators into nDSM analysis to extract building features. For this method, grayscale area morphological operation exhibited its efficiency for addressing large area building

extraction task. However, none effort is taken for consideration of the information loss problem.

In this paper, our contributions are: (1) A novel area morphological theory for 3-D airborne LiDAR point clouds rather than the rasterized 2-D image is proposed. (2) Based on the proposed area morphological operators, area morphological filtering framework for building extraction from airborne LiDAR data are given.

The rest of this paper is organized as follows: In Section II, at first, theory detail of the proposed area morphology for airborne LiDAR data is given, and then the corresponding area morphological filtering based building extraction method is described. In Section III, experiments for two airborne LiDAR data sets with different terrain characters are conducted. At last, some remarkable conclusions are given in Section IV.

2. Multi-scale 3D Area Morphological Filtering Based Building Extraction

2.1.3. D Area Morphology for Airborne LiDAR Point Clouds: For a given point clouds $\mathbf{P} = [\mathbf{X} \mathbf{Y} \mathbf{Z}] \in \mathbf{R}^{N \times 3}$ where N is the number of points, we can see it as a complete space Ω . In Ω , members of the *on-set* for a given height threshold h can be defined as $\mathbf{S}_h = \{\mathbf{p} = (x \ y \ z) | z \geq h\}$ and members of *off-set* can be defined as $(x, y, z) \in \mathbf{S}_h^c$ which is the complement of \mathbf{S}_h corresponding to the complete space Ω . With these basic definitions, there will be:

Definition 1: Connected. For any points pair $\mathbf{p}_1 = (x_1, y_1, z_1)$ and $\mathbf{p}_2 = (x_2, y_2, z_2)$ in Ω , if their Euclidean distance is smaller than a given threshold T_c , they are *connected*.

Definition 2: Connected component. For any points pair $\mathbf{p}_1 = (x_1, y_1, z_1)$ and $\mathbf{p}_2 = (x_2, y_2, z_2)$ from a same subset \mathbf{S}_i of \mathbf{S}_h , if there exists a connected path only includes members of \mathbf{S}_i between the two points. This subset \mathbf{S}_i is called connected component. Therefore, for a certain connected component \mathbf{S}_i , its area can be defined as the number of points in it. Therefore, $[\mathbf{S}_i]_{i \in \mathbf{I}}$ with \mathbf{I} being the indexes of connected components in \mathbf{S}_h can be used to represent *connected components* of \mathbf{S}_h .

Definition 3: Area opening operator. For the on-set \mathbf{S}_h , area opening operator can be used to remove all connected components \mathbf{S}_i with area less than a given threshold T_a :

$$\mathbf{S}_{Ta}^o(h) = \cup \{\mathbf{p} \in \mathbf{S}_i | Area(\mathbf{S}_i) \geq Ta\} \quad (1)$$

Definition 4: Area closing operator. For the off-set \mathbf{S}_h^c , area closing operator can be used to remove all connected components \mathbf{S}_i^c with area less than a given threshold T_a :

$$\mathbf{S}_{Ta}^c(h) = \cup \{\mathbf{p} \in \mathbf{S}_i^c | Area(\mathbf{S}_i^c) \geq Ta\} \quad (2)$$

Definition 5: Area opening-closing operator (AOC). AOC operator is defined by applying area opening followed by area closing with a given parameter T_a on the input point clouds.

Until now, let $\{h_j\}, j = 1, 2, \dots, N_h$ and $\{Ta_k\}, k = 1, 2, \dots, N_{Ta}$ be the parameter set to multi scale AOC operation. The corresponding scale-space $\{SP\}(\mathbf{P})$ can be formulated as below

$$\{SP\}(\mathbf{P}) \square \left\{ SP_k^j \mid SP_k^j = \mathbf{S}_{Ta_k}^c(h_j) \left(\mathbf{S}_{Ta_k}^o(h_j) (SP_{k-1}^j) \right) \right\} \quad (3)$$

where $SP_0^0 = \mathbf{P}$. Therefore, several connected regions can be extracted from the scale-space $\{SP\}(\mathbf{P})$.

For extracting building regions from candidates obtained by AOC operation on the input LiDAR data, region properties should be estimated to form rules. The mainly used rules for building region extraction are area or shape related. In order to obtain the corresponding properties, edges of the connected component should be defined at first. And before defining edge, neighborhood for connectivity analysis should be defined.

Definition 6: *8-directional-neighborhood*. For a given point $\mathbf{p} = [x \ y \ z] \in \mathbf{P}$, a local coordinate system $\mathbf{X}_L \mathbf{O}_L \mathbf{Y}_L$ can be established with (x, y) as the original point and with x and y axes paralleling to the corresponding axes directions of the object space coordinates. With the established coordinate system, *8-directional-neighborhood* can be defined as illustrated in Figure 1, where R is the scale of the defined *8-directional-neighborhood*.

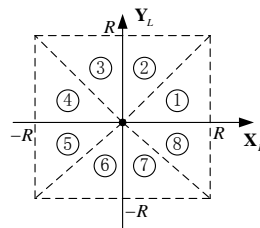


Figure 1. Illustration of the 8-Directional-Neighbor-Regions

Definition 7: *Edge point*. For a given point in one of the connected components $[S_i]_{i \in I}$ of S_h , if one of the following two conditions is satisfied, this point can be defined as an edge point belonging to S_i : (1) there is at least one of the 8-directional-neighborhood regions with none point in S_i ; (2) there is at least one of the 8-directional-neighborhood regions with the corresponding closest distance from neighbors in these regions to the center point is bigger than a given threshold E_s .

In Figure 2, connected components of a test LiDAR data with edges being highlighted were illustrated.

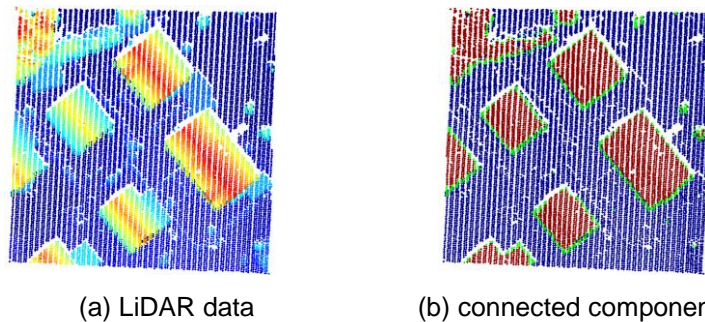


Figure 2. Illustration of Connected Components for a Real Airborne LiDAR Data Set

Besides area of a connected component, with the obtained edge points, several important geo-properties can also be obtained. (1) the number of edge points can be seen as *perimeter*. (2) The *area of minimum bounding rectangle* of the edge points. (3) the *linearity* of the edge points. (4) *main directions* of the edge points.

For obtaining the *linearity* and *main directions* of the edge points, starting from the first edge point e_1 , least square line fitting method can be used as below.

Step 1. Initializing n_s and n_b (the smallest and the biggest numbers of points to line fitting), the tolerance σ_l of line fitting error, the linearity vector $\mathbf{L}=\mathbf{O} \in \mathbf{R}^{n_s \times 1}$, and the direction vector $\mathbf{D}=\mathbf{O} \in \mathbf{R}^{n_b \times 1}$.

Step 2. For $u=1:n_e$ do

Let current scale be $n_l = n_b$,

While $\mathbf{L}(u)=0$ do

- getting all of the subsets composed of adjoining n_l edge points with current edge point \mathbf{e}_u in ;
- finding the best line fitting result with smallest fitting error ε_c , if ε_c is smaller than σ_l , the linearity of \mathbf{e}_u is $\mathbf{L}(u)=\exp(-\varepsilon_c)$ and the $\mathbf{D}(u)$ is assigned as the slope of the fitted line. Otherwise, $n_l = n_l - 1$.

While End.

Step 3. Find the first two main directions from direction vector.

Step 4. Stop.

With the corresponding connected components and their geo-properties described above, building extraction procedure can be conducted.

2.2. Area Morphological Filtering Based Building Extraction

With the proposed area morphological operators for airborne LiDAR point clouds, the diagram of building extraction procedure in this letter is illustrated in Figure 3.

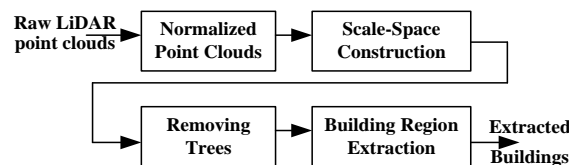


Figure 3. Diagram of Building Extraction Procedure

For building extraction, the raw LiDAR point clouds are firstly processed into normalized point clouds (nPC) which represent points with relative height to the 0 m flat terrain.

In order to obtain the nPC, AOC operator is employed in a sliding window way as below.

Step 1. Initializing the window size w , the sliding step ss , area threshold Ta for AOC operator, ground height vector $\mathbf{Gz}=\mathbf{Z} \in \mathbf{R}^{N \times 1}$, and $\mathbf{nPC}=\mathbf{P} \in \mathbf{R}^{N \times 3}$.

Step 2. Iterative ground fitting.

- With the upper-left point as the starting upper-left corner of data in the current window, let h be the median height of all of the points in current window.
- AOC operation is carried out.
- The height values of off-set points \mathbf{S}_h^c are used to fitting the terrain surface as

$$Z = P_{00} + P_{10}X + P_{01}Y + P_{11}XY + P_{20}X^2 + P_{02}Y^2 \quad (4)$$

- With the obtained fitting surface model, ground heights of the on-set points S_h can be calculated. For a certain point $\mathbf{p}_v \in S_h$, the corresponding value of $\mathbf{Gz}(v)$ will be

$$\mathbf{Gz}(v) = \min([\mathbf{Gz}(v), z_v^t]) \quad (5)$$

where z_v^t is the corresponding fitted ground heights for this point.

- Moving to the next window and do the steps above iteratively.

Step 3. Obtaining the final nPC with

$$\mathbf{nPC}(:,3) = \mathbf{nPC}(:,3) - \mathbf{Gz}. \quad (6)$$

With nPC data as input, the corresponding area morphology scale-space $\{SP\}(\mathbf{P})$ can be generated. In practice, the most important problem is to determine the configuration of the parameter set $\{h_j\}, j=1,2,\dots,N_h$ and $\{Ta_k\}, k=1,2,\dots,N_{Ta}$. For consideration that connected regions for a certain height scale are fixed for airborne LiDAR data in urban or suburb areas, result of AOC operation with bigger area scale is a subset of the corresponding result with smaller area scale. Therefore, for building region extraction, only one area scale is selected to contain as more as possible regions of the target buildings. In practice, this single scale can be selected as the area of the smallest building. And for the height scales, the corresponding values can be selected according to prior information about building heights of the test scene or can be selected from the local minima of the histogram of height values of nPC data (all of these local minima or a subset for reduce the computational burden).

With the determined parameter set for the area morphology scale-space generation, a series of binary point clouds with different number of connected components can be acquired. Obviously, in these connected components, there will be points from trees as false alarms. Therefore, change of curvature (COC) which is one of the most efficient PCA-based eigen-feature is employed to remove these tree points[3]. Specially, COC feature of any point \mathbf{p}_{ii} ($ii \in [1N] \subset \mathbf{Z}^1$) from the candidate building regions can be determined in the following way:

$$COC(\mathbf{p}_{ii}) = \min_{jj \in nbrinds} COC(\mathbf{p}_{jj}) \quad (7)$$

where $nbrinds$ is composed of indexes of the K nearest neighbors of point \mathbf{p}_{ii} . And jj is one of these indexes.

Therefore, candidate building regions can be extracted by analyzing rules derived from the corresponding geometry properties of connected regions of these binary images. The used geometry properties are: (1) *rectangularity* which is defined as the ratio of region area to the corresponding area of minimum bounding rectangle. (2) *compactness* which is defined as the region area divided by its perimeter. (3) *linearity* and (4) *main directions* which can be calculated as described in section II-B. And the used rules are:

$$rule1 = rectangularity \geq T_{rect}^1 \ \& \ compactness \geq T_{comp} \quad (8)$$

$$rule2 = rectangularity \geq T_{rect}^2 \ \& \ compactness \geq T_{comp} \ \& \ (linearity \geq T_{line} \ || \ main \ directions \approx \perp) \quad (9)$$

where $T_{rect}^1, T_{rect}^2, T_{comp}$, and T_{line} are four constant thresholds. The symbol \perp denotes perpendicular relationship between two angles. In this letter, the four constant thresholds are empirically set to be 0.75, 0.40, 3, and 0.45 respectively.

Therefore, for a given connected component: If *rule1* is true, it is taken as a candidate region; Otherwise, calculating *linearity* and *main directions*, if *rule2* is true it is also taken as a candidate region.

3. Experimental Results

3.1. Test Data sets

There are two airborne LiDAR data sets with different point densities and different terrain styles are used in this letter. The first data set (dataset1 which is illustrated in Figure 4. (b)) is a subset of ALS data collected for the USGS San Francisco Coastal LiDAR project. The corresponding horizontal and vertical accuracies are 2 m and 0.12 m respectively. Its point density is about 2 pts/m². And the area of this data set is about 177600 m², with 387110 LiDAR points. It can be seen that this region is an industrial zone with large variation of terrain slope and with several buildings connected with the foot of a high land in the scene. The second data set (dataset2 which is illustrated in Figure 4. (d)) is a subset of ALS data used for 2012 Data Fusion Contest. The corresponding standard deviation derived from the median of absolute deviation in the overlap areas is about 2.9 cm. Its point density is about 4 pts/m². And the area of this data set is about 61750 m², with 25 6650 LiDAR points.

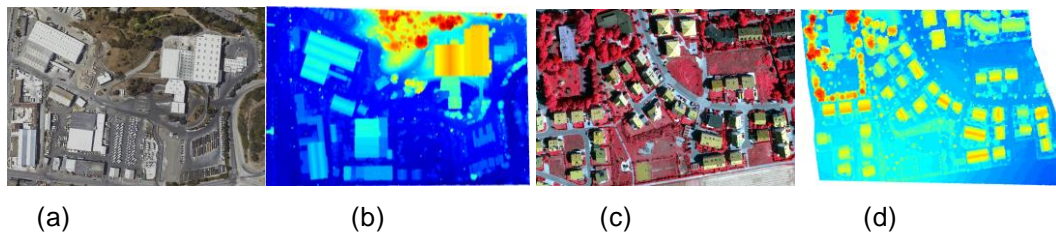


Figure 4. The Used raw LiDAR Data Sets: (a)-(b) are Optical Image and LiDAR Point Clouds of Dataset1; (c)-(d) are Optical Image and LiDAR Point Clouds of Dataset2

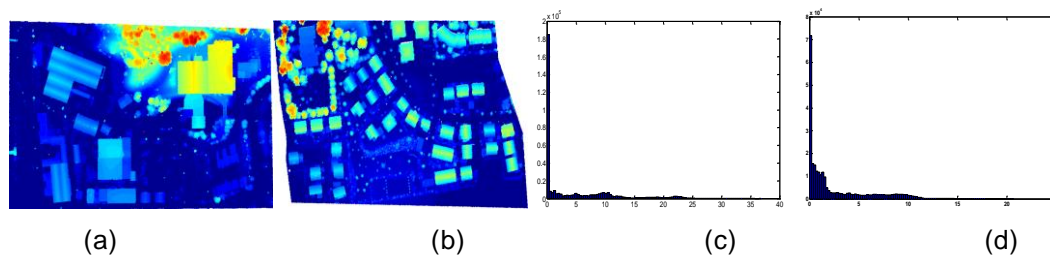


Figure 5. nPCs and the Corresponding Histograms of the Two Tests LiDAR DataS. (a)-(b) are nPCs of data set 1 and Data Set 2; (c)-(d) are Histograms of Data Set 1 and Data Set 2

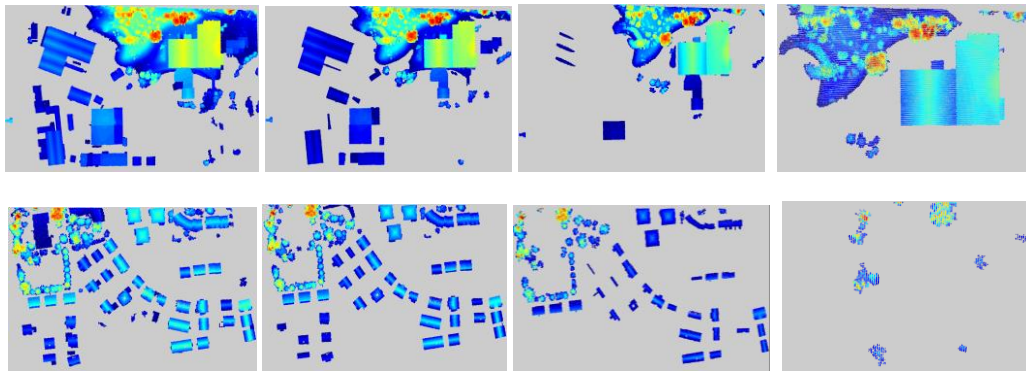


Figure 6. AOC Operation Results for the Two Data Sets.
The First Row are Results of Dataset1 and the
Second Row are Results of Dataset2.
(From Left to Right is Corresponding Results of the Finest Scale to the
Coarsest Scale)

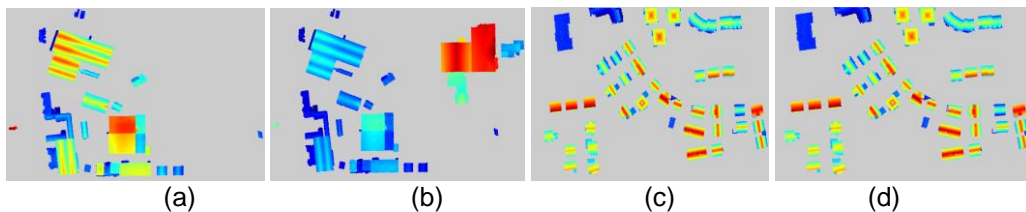


Figure 7. Building Extraction Results:
(a)-(b) Results of SS and MS Methods for Dataset1;
(c)-(d) Results of MS Methods for Dataset2.

3.2. Experimental Results

For evaluating the performance of the proposed method, two comparison methods were conducted. The first method is realized with only a single height scale (SS for short). The corresponding scale-space of the second method was constructed with multiple height scales (MS for short). For both of these two methods, raw LiDAR data sets should be transformed into nPCs at first (see Figure 5. (a)-(b)). And then, height scales should be determined. To release the computational burden, at most four height scales are used. Specially, in this letter, these height scales were acquired by analyzing local minima of histogram (100 bars) of the height values of nPC. For a given bar with its left 3 bars and right 3 bars as neighbors, if its value is the minimum of values of these neighbors, the corresponding center height value is treated as a candidate height scale. For the two data sets used, the corresponding histograms were illustrated in Figure 5. (c)-(d). The acquired height scales were [2.7609 7.1783 11.5957 14.5406] and [3.6200 5.2748 7.9639 12.7216], and the corresponding first value was selected for SS method as the height scale.

With the obtained height scales, AOC operation with area scale being 10 m² was applied with these height scales respectively. The corresponding AOC operation results were illustrated in Figure 6. And the final building extraction results of SS and MS methods were illustrated in Figure 7.

3.3. Accuracy Assessment and Discussion

To assess the accuracy of the proposed method, point-based evaluation was applied. At first, building points of the raw LiDAR data were manually labeled as reference data. Comparing with the reference data, true positive (TP), false positive (FP), and false

negative (FN) points were counted. With these values, correctness (*Corr*), completeness (*Comp*) and quality (*Qual*) are calculated as below:

$$Corr = \frac{TP}{TP + FN} \quad Comp = \frac{TP}{TP + FP} \quad Qual = \frac{TP}{TP + FN + FP}$$

The final results of these quantitative criteria for dataset1 and dataset2 were given in Table 1 and Table 2 respectively.

Table 1. Performance Comparison of SS and MS Building Extraction Method for data set 1

	TP	FN	FP	Correctness	Completeness	TotalQuality	Time (s)
SS	54957	23180	1984	0.7033	0.9652	0.6859	1548.52
MS	76474	1663	2090	0.9787	0.9734	0.9532	2965.29

Table 2. Performance Comparison of SS and MS Building Extraction Method for Data Set 2

	TP	FN	FP	Correctness	Completeness	TotalQuality	Time (s)
SS	42111	4330	1247	0.9068	0.9712	0.8831	1288.36
MS	42150	4291	1237	0.9076	0.9715	0.8841	2317.62

For dataset1, the corresponding terrain undulate is large. And there are large buildings at the root of a high land. Therefore, with only one height scale, SS method cannot extract buildings connected with the high land. As a result, we can see from Figure.7.(a)-(b) and Table 1 that the performance of SS method is much poorer than the corresponding results of MS method. On the other hand, by using multiple height scales, *Correctness*, *Completeness*, and *Quality* of MS method are all bigger than 0.95. For dataset2, the corresponding terrain is very flat. From Figure 7(c)-(d) and Table 2 we can see that the corresponding performance of SS and MS are almost the same. And both *Correctness* and *Completeness* are bigger than 0.9, the *Quality* is also bigger than 0.88. As to the computational efficiency, with Intel(R) Core(TM) i3-3220 CPU @ 3.30 GHz computer processor and 8 GB RAM memory, the proposed algorithms are developed using MATLAB R2012a. For dataset1, average time consumptions are 1548.52 s and 2965.29 s for SS and MS respectively. And for dataset2, the corresponding time are 1288.36 s and 2317.62 s. We can see that the proposed method is efficient for large scene processing.

4. Conclusions

In this paper, a very promising automatic building extraction framework for airborne LiDAR data is proposed by introducing area morphology idea into the raw LiDAR point clouds. The proposed method has high robustness to terrain character. By employing the proposed method with only one height scale, buildings in flattens area can be extracted efficiently. And the multi-scale solution of the proposed method can work well for scene with large terrain undulate.

Acknowledgement

The authors would like to thank USGS and the IEEE GRSS Data Fusion Technical Committee for providing the data sets used in this study.

References

- [1] H.G. Maas, G. Vosselman. "Two algorithms for extracting building models from raw laser altimetry data," *ISPRS Journal of P&RS*. vol. 54, (1999), pp. 153-163.
- [2] A. Sampath, J. Shan. "Segmentation and reconstruction of polyhedral building roofs from aerial LiDAR point clouds," *IEEE Trans. Geoscience and Remote Sensing.*, vol.48, no.3, (2010), pp.1554-1566.
- [3] F Tarsha Kurdi, T Landes, P Grussenmeyer. "Hough-transform and extended ransac algorithms for automatic detection of 3d building roof planes from lidar data," *International Archives of Photogrammetry, Remote Sensing and Spatial Information Systems.*, vol.36, (2007), pp.407-412.
- [4] E. Aparecida dos Santos Galvanin, A. Porfirio Dal Poz. "Extraction of building roof contours from LiDAR data using a Markov-Random-Field-Based approach," *IEEE Trans. Geoscience and Remote Sensing.*, vol. 50, no. 3, (2012), pp.981-987.
- [5] A. Sellaouti, A. Hamouda, A. Deruyver, and C. Wemmert. "Template-based hierarchical building extraction," *IEEE Geoscience and Remote Sensing Letters.*, vol.11, no. 3, (2014), pp. 706-710.
- [6] T. Thuy Vu, F. Yamazaki, and M. Matsuoka. "Multi-scale solution for building extraction from LiDAR and image data," *International Journal of Applied Earth Observation and Geoinformation.* vol.11, (2009), pp.281-289.
- [7] Y. Ioannou, B. Taati, and R. Harrap. "Difference of Normals as a Multi-scale operator in unorganized point clouds," in *Second Joint 3DIM/3DPVT conference*, Seattle, USA, (2012), pp.501-508.
- [8] N. Brodu, D. Lague, "3D terrestrial lidar data classification of complex nature scenes using a multi-scale dimensionality criterion: Applications in geomorphology," *ISPRS Journal of P&RS.*, vol.68, (2012), pp.121-134.
- [9] E.H Lim, S. David. "Multi-scale conditional random fields for over-segmented irregular 3D point clouds classification," in *CVPRW'08*, Anchorage, AK, (2008), pp.1-7.
- [10] M.K. Park, S.J. Lee, and K.H. Lee, "Multi-scale tensor voting for feature extraction from unstructured point cloud," *Graphical Models.*, vol.74, (2012), pp.197-208.

Authors



Cao Zhimin received the B.S. degree in electronic information engineering from Daqing Petroleum Institute, Daqing, Heilongjiang, China, in 2003, and the M.S. degree in Information and Communication Engineering from Harbin Institute of Technology, Harbin, Heilongjiang, China, in 2008, where he is currently working toward the Ph.D. degree in the School of Electronic and Information Engineering. He is currently a lecturer in School of Electronic Science in North-East Petroleum University, Daqing, Heilongjiang, China. His research interest includes airborne LiDAR data processing and application, 3D reconstruction, *et al.*



Wu Yun received the B.S. degree in electronic information engineering from Daqing Petroleum Institute, Daqing, Heilongjiang, China, in 2002, and the M.S. degree in Measuring and Testing Technologies and Instruments in North-East Petroleum University, Daqing, Heilongjiang, China, in 2008. She is currently working toward the Ph.D. degree in the School of Colledge of Underwater Acoustic Engineering. She is currently an associate professor in School of Electronic Science in North-East Petroleum University, Daqing, Heilongjiang, China. Her research interest includes image processing and pattern recognition, underwater acoustic signal processing, and *et al.*

